Current CRISPR gene drive systems are likely to be highly invasive in wild populations

Charleston Noble[1,2,3,*], Ben Adlam[1,4,*], George M. Church[2,3], Kevin M. Esvelt[5,†], Martin A. Nowak[1,6,7,†]

[1]Program for Evolutionary Dynamics, Harvard University, Cambridge, MA
[2]Department of Genetics, Harvard Medical School, Harvard University, Boston, MA
[3]Wyss Institute for Biologically Inspired Engineering, Harvard University, Boston MA
[4]School of Engineering and Applied Science, Harvard University, Cambridge MA
[5]Massachusetts Institute of Technology Media Lab, Cambridge, MA
[6]Department of Mathematics, Harvard University, Cambridge, MA
[7]Department of Organismic and Evolutionary Biology, Harvard University, Cambridge, MA
[*]These authors contributed equally to this work.
[†]Correspondence to martin_nowak@harvard.edu (M.A.N.), esvelt@mit.edu (K.M.E.)

Abstract

Recent reports have suggested that CRISPR-based gene drives are unlikely to invade wild populations due to drive-resistant alleles that prevent cutting. Here we develop mathematical models based on existing empirical data to explicitly test this assumption. We show that although resistance prevents drive systems from spreading to fixation in large populations, even the least effective systems reported to date are highly invasive. Releasing a small number of organisms often causes invasion of the local population, followed by invasion of additional populations connected by very low gene flow rates. Examining the effects of mitigating factors including standing variation, inbreeding, and family size revealed that none of these prevent invasion in realistic scenarios. Highly effective drive systems are predicted to be even more invasive. Contrary to the National Academies report on gene drive, our results suggest that standard drive systems should not be developed nor field-tested in regions harboring the host organism.

Introduction

CRISPR-based gene drive systems can bias inheritance of desired traits by cutting a wild-type allele and copying the drive system in its place[1]. Following reports of successful CRISPR gene drive systems in yeast[2] and fruit flies[3], scientists emphasized the need to employ strategies beyond traditional barrier containment as a laboratory safeguard[4,5]. These precautions were judged necessary to prevent unintended ecological effects, but also because any unauthorized release affecting a wild population could severely damage trust in scientists and governance, significantly delaying or even precluding applications of gene drive and other biotechnologies.

Drive resistance can result from mutations that block cutting by the CRISPR nuclease. Recent examinations of the phenomenon by experiments and deterministic models have generated substantial media attention[6–9]. Resistance can arise from standing genetic variation at the drive locus or because the drive mechanism is not perfectly efficient and is predicted to prevent drive fixation in wild populations unless additional mitigating strategies are employed[1,9–12].

Recent articles highlighting the problem of resistance for gene drives have suggested that resistance will prevent drive invasion in wild populations—with some even implying that resistance could serve as an experimental safeguard. While resistance should prevent drive fixation, an allele can nonetheless spread to significant frequency without fixing. To clarify this point, we

sought to quantify the likelihood and magnitude of spread in the most likely unauthorized release scenario—a small number of engineered individuals released into a wild population.

CRISPR gene drive systems function by converting drive-heterozygotes into homozygotes in the late germline or early embryo[1] (Figure 1A). First, a CRISPR nuclease encoded in the drive construct cuts at the corresponding wild-type allele—its target prescribed by an independently expressed guide RNA (gRNA)—producing a double-strand break[13]. This break is then repaired either through homology-directed repair, producing a second copy of the gene drive construct, or through a nonhomologous repair pathway (non-homologous end joining, NHEJ, or microhomology-mediated end joining, MMEJ), which typically introduces a mutation at the target site[14,15]. Because the drive target is determined through sequence homology, such a mutation generally results in resistance to future cutting by the gene drive. Thus, the allele converts from a wild-type to resistant allele if it undergoes repair by a pathway other than homology-directed repair. Moreover, drive-resistant alleles are expected to exist in wild populations simply due to standing genetic variation[7,8].

Deterministic models, which assume an infinite, well-mixed population, predict whether an allele is initially favored by selection, i.e., favored to increase in frequency when initially rare in a wild population[16]. Whether gene drives are initially favored by selection depends on two key parameters: the *homing efficiency (P)*, or the probability of undergoing homology-directed repair instead of nonhomologous repair, and *fitness (f)*, or the relative fecundity or death rate the drive and its cargo confer on their organism compared to the wild-type. Mathematically, drives are initially favored by selection if $f(1+P)>1$, i.e., if the inheritance bias of the drive exceeds its fitness penalty[9,11,17]. Given that the homing efficiencies of reported drive systems typically range from 0.37 to 0.99 (Table S1), current drive systems can clearly be initially favored by selection. Although the fitness parameter, f, is typically not measured in proof-of-concept studies, a substantial fitness cost is tolerable by all reported CRISPR drive constructs[6,2,3,18,19] (Figure 1B).

However, in finite populations, the fate of initially rare alleles is determined not only by selection but also by stochastic fluctuations[20–22]. Therefore, stochastic models are required to predict the probability that a drive spreads to some preset frequency when they are initially favored by selection. A previous, and arguably prescient, stochastic model of endonuclease drive containment found that homing-based drives, such as those subsequently developed using CRISPR, were among the likeliest to invade of the various drive alternatives[23]. To determine whether drives are still able to invade in the presence of resistance, we formulated a finite population, stochastic, Moran-based model that allows us to study small releases in finite and structured populations (Methods).

Results

Our model considers three distinct allelic classes: wild-type (W), gene drive (D), and resistant (R). Consistent with experiments, we assume that the drive invariably cuts the wild-type allele in the germline of a heterozygous WD individual, converting to a drive allele with probability P, or a resistant allele with probability $1-P$. Each genotype, AB, has a relative reproductive rate, f_{AB}, corresponding to its fitness in deterministic models, normalized such that the wild-type homozygote has fitness one ($f_{WW}=1$), the drive confers a dominant cost ($f_{DW}=f_{DD}=f_{DR}<1$), and resistance is neutral ($f_{RR}=1$). This ordering of the parameters represents the worst-case scenario for drive spread (SI Section 2.6).

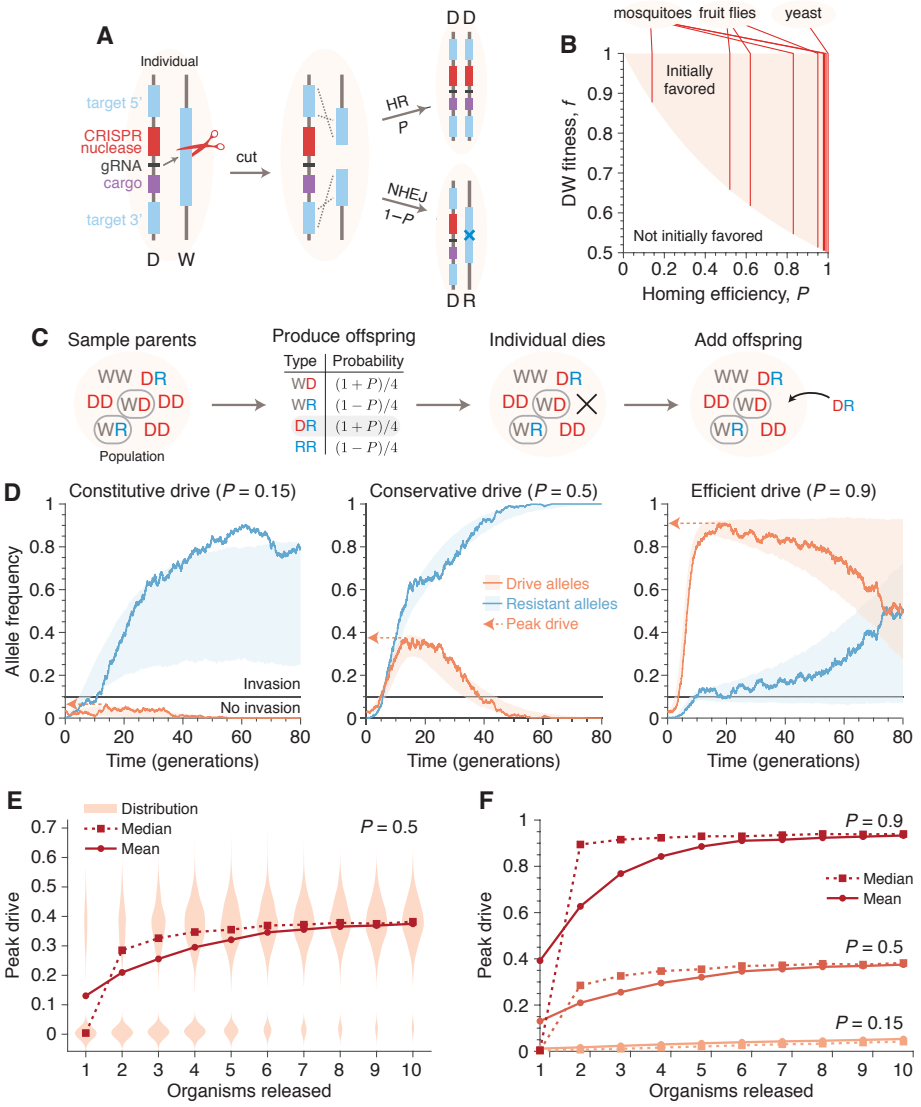

Figure 1. Existing CRISPR gene drive systems should invade well-mixed wild populations. (A) Typical construction and function of CRISPR gene drive systems. A drive construct (D), including a CRISPR nuclease, guide RNA (gRNA), and "cargo" sequence, induces cutting at a wild-type allele (W) with homology to sequences flanking the drive construct. Repair by homologous recombination (HR) results in conversion of the wild-type to a drive allele, or repair by nonhomologous end-joining (NHEJ) produces a drive-resistant allele (R). (B) Drives are initially favored by selection when the fitness of DW heterozygotes, f, and the homing efficiency, P, are in the shaded region. Vertical lines indicate empirical efficiencies from Table S1. (C) Diagram of a single step of the gene-drive Moran process. (D) Finite-population simulations of 15 drive individuals released into a wild population of size 500, assuming conservative (P=0.5) or high (P=0.9) homing efficiencies, as well as a low-efficiency, constitutively active system (P=0.15). Individual sample simulations (solid lines), and 50% confidence intervals (shaded), calculated from 10^3 simulations. Drive-allele frequencies red and resistant-allele frequencies blue. *Peak drive*, or maximum frequency reached, is illustrated by dashed lines and arrows. We say that a drive *invades* if its peak is greater than 0.1. (E) Peak drive distributions as a function of the number of organisms released (P=0.5). (F) Means (solid lines) and medians (dotted) of peak drive distributions for varying homing efficiencies (P=0.15, bottom; P=0.5, middle; P=0.9, top). Throughout, we assume neutral resistance (f_{WR}=f_{DR}=f_{RR}=1) and a 10% dominant drive fitness cost (f_{WD}=f_{DD}=f_{DR}=0.9).

At the population level, our basic model considers N diploid individuals mating randomly. The process unfolds in discrete steps, during which parents are chosen for reproduction, an offspring is chosen according to the mechanism above, and another individual is replaced by the offspring (Figure 1C and Methods). These steps are repeated until one allele fixes. A *generation* is N time-steps, which corresponds to the mean lifespan of an individual.

Figure 1D shows typical simulations for drive efficiencies of 0.15, 0.5, and 0.9, which correspond respectively to a constitutively active drive system targeting a common insertion site, and conservative and high efficiency systems (based on previous experimental studies, Table S1, Figure 1B, SI Section 1). These simulations assume a dominant drive fitness cost of 10%, a population of size 500, and a release of 15 drive-homozygous individuals. (Note that the dynamics are similar for larger population sizes; see SI Section 2.1 and Figure S1.) In all three cases, the drive, on average, irreversibly alters a majority of the population, either via invasion of the drive itself or via spread of drive-created resistant alleles. We call the maximum frequency of drive alleles reached during a simulation the *peak drive*, and we say a drive has *invaded* if it reaches a frequency of 0.1. Importantly, although arbitrary, the choice of 0.1 is large enough to ensure peak drive on par with deterministic models (SI Section 2.6 and 2.7). Invasion is very unlikely when the drive is not initially favored by selection.

We next calculated the distribution of peak drive while varying the number of organisms released (Figs. 1e and 1f). We find that these distributions are bimodal, with one mode centered around the initial frequency (corresponding to drift leading rapidly to extinction) and one centered roughly around the maximum values observed in the large-release scenarios in Figure 1D. The former mode shrinks rapidly as more organisms are released, and for the parameters studied, a release of 10 individuals nearly guarantees invasion with substantial peak drive (SI Section 2.6, Figure S7).

To understand the extent to which isolation might prevent invasion of other populations connected by gene flow, we introduced population structure. Our model consists of five subpopulations (or islands) that are equally connected by migration (Figs. 2a and SI Section 7, Methods). Typical dynamics are illustrated in Figure 2C. Figures 2B and 2D show the *escape probability*, or the probability of the drive invading (attaining a frequency of 0.1) at least one subpopulation other than its originating one, and Figure 2E shows the probability of invading a varying number of subpopulations.

Our results in Figure 2 suggest that if the migration rate is extremely low, then the drive is effectively contained in the initial subpopulation. If the migration rate is high, the drive is almost guaranteed to invade all subpopulations linked to the originating one. For intermediate migration rates—characterized roughly by migration rates on the order of the inverse of the drive extinction time—both outcomes occur. In the scenario studied in Figure 2, a migration rate of 10^{-3}, which corresponds to a single migration event every 2 generations on average (Methods), virtually guarantees escape for moderate drive efficiencies (Methods). For further details and analytical formulae allowing rapid estimation of escape probabilities, see SI Section 2.7.

Finally, we sought to understand the effects of additional mitigating factors that could potentially affect peak drive or invasion. We considered the most prominent factors that have arisen in previous papers, and we studied each by varying parameters in our basic model and developing model extensions. Our results are explored in detail in the Supplementary Information (Section 3).

First, we considered preexisting drive resistance resulting from standing genetic variation[7,8] (SI Section 2.2). We find that increasing the proportion of the population that is initially resistant linearly decreases the mean peak drive (R^2=0.996). Using the parameters in Figure 1E

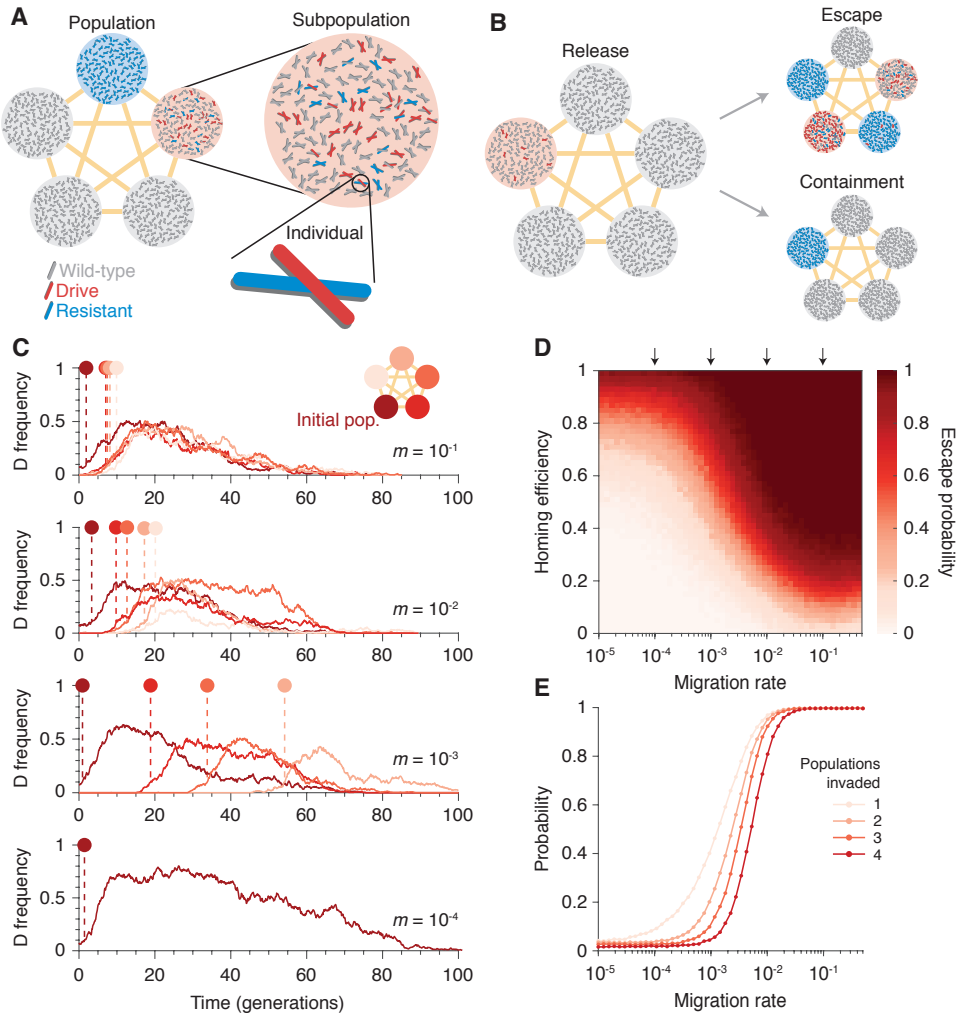

Figure 2. Existing CRISPR gene drive systems should invade linked subpopulations connected by gene flow. (A) Diagram of well-mixed subpopulations (circles) linked by gene flow (edges). Individuals represented by chromosomes with wild-type (gray), drive (red), or resistant (blue) haplotypes. (B) Few drive homozygotes are released in one subpopulation. The drive *escapes* if it invades another subpopulation before going extinct. Otherwise it is *contained*. (C) Typical simulations for varying migration rates (m=10^{-1}, top, to m=10^{-4}, bottom), following introduction into a single subpopulation. Lines represent drive frequencies in each subpopulation. Circles correspond to the time the drive invades a subpopulation. (D) Escape probability as a function of homing efficiency, P, and migration rate, m. Arrows indicate migration rates from B. Each pixel is calculated from 10^3 simulations. (E) Probability of invading 1, 2, 3, or 4 populations (aside from the originating population), assuming a homing efficiency of P=0.5. Each data point is calculated from 10^4 simulations. Throughout, we consider 5 subpopulations connected in a complete graph, each consisting of 100 individuals. Initially, 15 drive homozygotes are introduced into one subpopulation. Resistance is neutral (f_{WR}=f_{DR}=f_{RR}=1) and the drive confers a dominant 10% cost (f_{WD}=f_{DD}=f_{DR}=0.9).

and considering a release of 15 individuals, more than 50% preexisting resistance is required to contain average peak drive below 10% (Figure S2).

Second, we studied the effect of varying family size, which may be relevant to species such as mosquitoes with large egg batch sizes[19,24]. We extended the model so that k (adult) offspring are produced from a reproduction event, rather than one. We find that this effect scales the release and population sizes[25] by a factor of $4/(2k+6)$. For illustration, we estimated k for *Anopheles gambiae* to be roughly 10 (SI Section 2.3), so that a release of 7 individuals roughly corresponds to a release of 1 individual in our basic model. While this effect somewhat reduces the chance of drive invasion for small release sizes, it does not preclude it.

Third, we varied fitness and homing efficiency across the regime where the drive is initially favored by selection (Figure 1B) and recorded peak drive (SI Section 2.4, Figure S5). We find that peak drive is on average greater than 30% across the majority of the regime and almost always greater than 10%.

Fourth, we studied the effect of inbreeding, which has been shown in several recent theoretical studies[26,8] to impede drive spread (SI Section 2.5). We extended the model to include a probability s of an individual selfing rather than mating with a second individual[26]. The model assumes no inbreeding depression and thus considers the worst-case scenario for drive[26]. We find that even in this scenario, high selfing probabilities are required to reduce peak drive and the probability of invasion for moderate drive costs.

There are a variety of other phenomena that could affect invasiveness, e.g., density dependence[27], environment[28], costly resistance[29], local ecology, and even mating incompatibilities between some laboratory strains and wild individuals. Such effects should be carefully studied in subsequent papers. Most importantly, the drive architecture itself should affect invasiveness; we consider here only alteration-type drive systems, while others, e.g., sex-ratio distorters and genetic load drives, would be expected to yield different dynamics. In particular, population suppression drive systems may locally self-extinguish before invading new populations. However, for alteration drives, our key qualitative finding—that peak drive is difficult to reliably contain below a socially tolerable threshold following a very small release of organisms—appears robust to a variety of mitigating factors. Fundamentally, we exercise caution by omitting application-specific phenomena that might aid containment in particular instances but not in general.

Discussion

Our results suggest that current first-generation CRISPR gene drive systems are capable of far-reaching—perhaps, for species distributed worldwide, global—spread, even for very small releases. A simple, constitutively expressed CRISPR nuclease and guide RNA cassette targeting the neutral site of insertion—an arrangement that could occur accidentally—may be capable of altering many populations of the target species depending on the homing efficiency of the organism in question. More generally, resistance can be problematic for intentional applications of gene drives, but we find that it is not a major impediment to invasion of unintended populations.

Our results have numerous implications for future gene drive research. First, researchers interested in studying self-propagating gene drives may wish to refrain from constructing systems that are capable of invading wild populations. Invasion can be avoided by employing intrinsic molecular confinement mechanisms such as synthetic site targeting or split drive, as recommended by the National Academies[4]. Second, contrary to the National Academies' recommendation of a staged testing strategy, the predicted invasiveness of current CRISPR-based drive systems may

preclude field trials, possibly even on ostensibly isolated islands. The development of 'local', intrinsically self-exhausting gene drive systems[30–34], sensitive methods of monitoring population genetics, and strategies for countering self-propagating drive systems and restoring populations to wild-type should be a correspondingly high priority.

Methods

Well-mixed finite population model

To model gene drives in finite populations, we introduce a Moran-type model with sexual reproduction (illustrated in Figure 1C). We consider a population of N individuals, each of which is diploid. We focus on a locus with three allelic classes: wild-type (W), CRISPR gene drive element (D) and drive-resistant (R). There are six possible genotypes: WW, WD, WR, DD, DR, and RR. We assign to each genotype α a reproductive rate f_α.

The process proceeds in discrete time-steps, during each of which three events occur in succession (Figure 1C). First, two individuals are chosen without replacement for mating with probabilities proportional to their reproductive rates, so that genotype α is selected with probability

$$\frac{f_\alpha N_\alpha}{\sum_\beta f_\beta N_\beta}.$$

Here N_α is the number of individuals having genotype α, and the sum in the denominator is over all six genotypes. Second, after selecting the two parents, the offspring genotype is chosen randomly based on the genotypes of the two parents. To proceed, we introduce notation $\alpha = AB$ to mean that genotype α consists of alleles A and B, and we index these alleles via $\alpha_1 = A$ and $\alpha_2 = B$. Note that we track only one genotype for each heterozygote, implicitly combining counts for genotypes AB and BA. Using this notation, the probability that an offspring of genotype γ is chosen given a mating between parents of genotypes α and β is given by the quantity $q^\gamma_{\alpha\beta}$, which is equal to

$$\frac{q_\alpha^{\gamma_1} q_\beta^{\gamma_2} + q_\alpha^{\gamma_2} q_\beta^{\gamma_1}}{1 + \delta_{\gamma_1\gamma_2}}$$

Here q^A_α is a gamete production probability—the probability that a parent with genotype α produces a gamete with haplotype A—and δ_{AB} is the Kronecker delta, defined by $\delta_{AB} = 1$ if $A = B$ (i.e., if the offspring under consideration is a homozygote), and $\delta_{AB} = 0$ otherwise. The gamete production probabilities, q^A_α, are determined by accounting for the gene drive process described in the main text. They are given by: $q^W_{WW} = q^D_{DD} = q^R_{RR} = 1$, $q^D_{WD} = (1+P)/2$, $q^R_{WD} = (1-P)/2$, $q^W_{WR} = q^R_{WR} = q^D_{DR} = q^R_{DR} = 1/2$. The remaining values not listed, e.g., q^R_{WW}, are zero. Third, an individual is chosen uniformly at random for death. Thus, the population size remains constant. The resulting counts become the starting abundances for the next iteration of the process. The process is initialized with a small number, i, of drive homozygotes (DD) and the remaining population, $N - i$, wild-type homozygotes (WW). The process continues as described above either until a specified number of time steps have elapsed or until one of the three alleles has fixed. Any of the alleles can fix, but typically either the wild-type or resistant alleles fix, due to the emergence of resistance.

Finite population model with population structure

To study the effects of population structure on drive containment, we extended the well-mixed model from the previous section. We now consider l well-mixed subpopulations, each consisting initially of N/l individuals. The process proceeds in discrete time steps, as before. In each time

step, we either migrate an individual from one population to another, or we choose a particular subpopulation and proceed through one mating and replacement iteration, as outlined above. More specifically, one step of the process proceeds as follows (illustrated in Figure S8). With probability m, we initiate a migration event. In this case, we perform three steps. First, we choose a source population with probability proportional to its size. Second, we choose an individual uniformly at random from the source population for migration. Finally, we move the chosen individual to a linked subpopulation uniformly at random. Or, with probability $1 - m$, we initiate a mating event as described in the well-mixed section. To carry this out, we first choose the population in which the event will occur. We choose this population with probability proportional to the square of its total fitness. We then step through one iteration of the well-mixed mating process within this sub-population. Note that in this model the migration rate has a simple interpretation. The time between migrations is geometrically distributed with parameter m, so the mean time between migrations is $1/m$ time steps. Recall that a "generation" is equal to the mean lifespan of an individual, that is, N reproduction events or $N/(1-m)$ time steps. Then the typical time between migrations can be expressed with the units as generations:

$$E[T] = \frac{1-m}{Nm}.$$

Deterministic model

To compare our stochastic simulations with deterministic results, we use a recently published model[9]. From that work, we employ the "previous drive" model, as it was designed to agree with the existing proof-of-concept CRISPR drive constructs that we consider here. Specifically, we consider the case of 1 guide RNA ($n = 1$ in that work's notation), and zero production of costly resistant alleles ($\gamma = 1$).

References

1. Esvelt, K. M., Smidler, A. L., Catteruccia, F. & Church, G. M. Concerning RNA-guided gene drives for the alteration of wild populations. *Elife* **3,** e03401 (2014).
2. DiCarlo, J. E., Chavez, A., Dietz, S. L., Esvelt, K. M. & Church, G. M. Safeguarding CRISPR-Cas9 gene drives in yeast. *Nat. Biotechnol.* (2015). doi:10.1038/nbt.3412
3. Gantz, V. M. & Bier, E. The mutagenic chain reaction: A method for converting heterozygous to homozygous mutations. *Science* **348,** 442–444 (2015).
4. National Academies of Sciences, Engineering, and Medicine. *Gene Drives on the Horizon: Advancing Science, Navigating Uncertainty, and Aligning Research with Public Values*. (National Academies Press, 2016).
5. Akbari, B. O. S. *et al.* Safeguarding gene drive experiments in the laboratory. *Science* **349,** 927–9 (2015).
6. Champer, J. *et al.* Novel CRISPR/Cas9 gene drive constructs reveal insights into mechanisms of resistance allele formation and drive efficiency in genetically diverse populations. *PLOS Genet.* **13,** e1006796 (2017).
7. Unckless, R. L., Clark, A. G. & Messer, P. W. Evolution of Resistance Against CRISPR/Cas9 Gene Drive. *Genetics* **205,** 827–841 (2017).
8. Drury, D. W., Dapper, A. L., Siniard, D. J., Zentner, G. E. & Wade, M. J. CRISPR/Cas9 gene drives in genetically variable and nonrandomly mating wild populations. *Sci. Adv.* **3,** (2017).
9. Noble, C., Olejarz, J., Esvelt, K. M., Church, G. M. & Nowak, M. A. Evolutionary dynamics of CRISPR gene drives. *Sci. Adv.* **3,** (2017).
10. Burt, A. Site-specific selfish genes as tools for the control and genetic engineering of natural populations. *Proc. Biol. Sci.* **270,** 921–928 (2003).

11. Deredec, A., Burt, A. & Godfray, H. C. J. The population genetics of using homing endonuclease genes in vector and pest management. *Genetics* **179,** 2013–2026 (2008).
12. Marshall, J. M., Buchman, A., Sánchez C., H. M. & Akbari, O. S. Overcoming evolved resistance to population-suppressing homing-based gene drives. *Sci. Rep.* **7,** 3776 (2017).
13. Jinek, M. *et al.* A programmable dual-RNA-guided DNA endonuclease in adaptive bacterial immunity. *Science* **337,** 816–21 (2012).
14. Mali, P. *et al.* RNA-guided human genome engineering via Cas9. *Science* **339,** 823–6 (2013).
15. Cong, L. *et al.* Multiplex genome engineering using CRISPR/Cas systems. *Science* **339,** 819–23 (2013).
16. Nowak, M. A. *Evolutionary Dynamics*. (Harvard University Press, 2006).
17. Unckless, R. L., Messer, P. W., Connallon, T. & Clark, A. G. Modeling the manipulation of natural populations by the mutagenic Chain reaction. *Genetics* **201,** 425–431 (2015).
18. Gantz, V. M. *et al.* Highly efficient Cas9-mediated gene drive for population modification of the malaria vector mosquito Anopheles stephensi. *Proc. Natl. Acad. Sci.* 201521077 (2015). doi:10.1073/pnas.1521077112
19. Hammond, A. *et al.* A CRISPR-Cas9 gene drive system targeting female reproduction in the malaria mosquito vector Anopheles gambiae. *Nat. Biotechnol.* (2015). doi:10.1038/nbt.3439
20. Wright, S. Evolution in Mendelian populations. *Genetics* **16,** 97–159 (1931).
21. Fisher, R. *The genetical theory of natural selection*. (The Clarendon Press, 1930).
22. Haldane, J. B. S. A mathematical theory of natural and artificial selection. Part V. Selection and mutation. *Proc. Camb. Phil. Soc* **23,** 838–844 (1927).
23. Marshall, J. M. The effect of gene drive on containment of transgenic mosquitoes. *J. Theor. Biol.* **258,** 250–265 (2009).
24. Yaro, A. S. *et al.* Reproductive Output of Female Anopheles gambiae (Diptera: Culicidae): Comparison of Molecular Forms. *J. Med. Entomol.* **43,** 833–839 (2006).
25. Hill, W. G. Effective size of populations with overlapping generations. *Theor. Popul. Biol.* **3,** 278–289 (1972).
26. Bull, J. J. Lethal gene drive selects inbreeding. *Evol. Med. Public Heal.* eow030 (2016). doi:10.1093/emph/eow030
27. Deredec, A., Godfray, H. C. J. & Burt, A. Requirements for effective malaria control with homing endonuclease genes. *Proc. Natl. Acad. Sci. U. S. A.* **108,** E874-80 (2011).
28. Tanaka, H., Stone, H. A. & Nelson, D. R. Spatial gene drives and pushed genetic waves. *arXiv:1704.03525* (2017). doi:10.1101/126722
29. Traulsen, A. & Reed, F. A. From genes to games: Cooperation and cyclic dominance in meiotic drive. *J. Theor. Biol.* **299,** 120–125 (2012).
30. Chen, C. *et al.* A Synthetic Maternal-Effect Selfish Genetic Element Drives Population Replacement in Drosophila. *Science* **316,** 597–600 (2007).
31. Akbari, O. S. *et al.* Novel Synthetic Medea Selfish Genetic Elements Drive Population Replacement in Drosophila; a Theoretical Exploration of Medea -Dependent Population Suppression. *ACS Synth. Biol.* **3,** 915–928 (2014).
32. Noble, C. *et al.* Daisy-chain gene drives for the alteration of local populations. *bioRxiv* (2016). doi:10.1101/057307
33. Magori, K. & Gould, F. Genetically engineered underdominance for manipulation of pest populations: a deterministic model. *Genetics* **172,** 2613–20 (2006).
34. Gould, F., Huang, Y., Legros, M. & Lloyd, A. L. A killer-rescue system for self-limiting gene drive of anti-pathogen constructs. *Proc. Biol. Sci.* **275,** 2823–9 (2008).

Acknowledgments

We thank J. Wakeley for helpful discussions. C.N. received support from the NSF Graduate Research Fellowship Program under grant no. DGE1144152. K.M.E. was supported by the Burroughs Wellcome Fund (IRSA 73786).

Author contributions

K.M.E. and M.A.N. conceived the study. C.N., B.A. and M.A.N. created the mathematical models, and all authors analyzed the results. C.N. and B.A. wrote the manuscript with contributions from all authors.

Supplementary Information: Current CRISPR gene drive systems are likely to be highly invasive in wild populations

Charleston Noble*, Ben Adlam*,
George M. Church, Kevin M. Esvelt†, Martin A. Nowak†

In this Supplementary Information, we first describe in Section 1 the empirical data reviewed for determining the homing efficiencies depicted in Fig. 1b. These results are summarized in Table S1. Then in Section 2, we further analyze our mathematical model for gene drive in finite populations.

1 Empirical data

In Table S1, we present empirical homing efficiencies for all CRISPR gene drive constructs reported to date. These studies varied in multiple ways: they studied different organisms; they used different methods for counting drive constructs (ranging from direct genetic measurement, such as quantitative PCR, to indirectly observing visible phenotypes), and they sometimes observed differential inheritance rates between sexes, possibly due to differences in male and female gamete characteristics. Given this complexity, we elaborate here on the specific data we selected for review to produce Table S1 and the reasoning for our choices.

To begin, all studies performed some variation of producing drive/wild-type heterozygotes (DW), followed by counting the number which converted their wild-type allele to a drive allele. There were two main approaches.

1. Some constructs acted in the early embryo, in which case WW and DD individuals were mated to produce offspring which were initially WD. Observations were then made of adult genotypes. DD individuals must have undergone drive conversion, while WD individuals must have avoided conversion. Without drive, all adults are expected to be WD, but with drive, all are expected to be DD.

2. Other constructs acted in the germline of adults, so that adult WD individuals produce D gametes more often than chance under the effects of drive. To study these constructs, WD individuals were mated with WW individuals. Without drive, half of adults should be WW, and half should be WD. With drive, however, all adults should be WD.

To employ a consistent strategy across the studies, we calculate two numbers for each drive construct: (i) the total number of initial alleles counted which were drives or were subject to drive, T, and (ii) the total number of resulting drive alleles, D. The homing efficiency can then be calculated in the following way:

$$P = \frac{2D}{T} - 1$$

*These authors contributed equally to this work.
†Correspondence to martin_nowak@harvard.edu (M.A.N.), esvelt@mit.edu (K.M.E.)

Organism	Ref.	System name	Efficiency
Yeast	[1]	ade2::sgRNA	$> 99\%$
		ade2::sgRNA+URA3	100%
		sgRNA+ABD1	100%
		cas9+sgRNA	$> 99\%$
		ADE2+sgRNA+cas9	$> 99\%$
Fruit flies	[2]	γ-MCR	95%
	[3]	nanos	62%
		vasa	52%
		additional nanos	40%–63%
		additional vasa	37%–53%
Mosquitoes	[4]	AsMCRkh2 (male)	98%
		AsMCRkh2 (female)	14%
	[5]	AGAP011377	83%
		AGAP005958	95%
		AGAP007280	99%

Table S1: Empirical homing efficiencies for all CRISPR gene drive systems published to date. Details can be found in SI Section 1.

Notice that if drive is perfectly efficient ($P = 1$), we have $D/T = 1$, *i.e.*, there are twice as many drive alleles as starting heterozygotes, while under standard inheritance ($P = 0$), the number of drive alleles is unchanged from the initial heterozygous state, $D/T = 1/2$. Below, we explain our calculations of these quantities for Table 1.

Yeast, DiCarlo et al., (2015)

The study by DiCarlo et al. studied 5 distinct gene drive systems in yeast [1]. We address each distinct system in subsections below.

1. ade2::sgRNA

This is the basic split drive system containing only a guide RNA. Its design is depicted in Fig. 2B, and it is described on pp. 1250-1251, with results pictured in Fig. 2D and Fig. 4. Drive abundances were measured via colony counting (Fig. 2D), obtaining absolute colony numbers, and via qPCR (Fig. 4), obtaining relative abundances of drive alleles. By the colony counting method, the drive efficiency is measured at 100% ($D = T = 72$). By the qPCR method, $> 99\%$ of alleles counted from offspring were drive alleles, so $D > 0.99T$. Therefore:

$$P > 0.99$$

Strictly speaking, the inequality $D > 0.99T$ entails $P > 0.98$, but we set this to $P > 0.99$ because the qPCR results were indistinguishable from 100%. We make a similar approximation below for systems 4 and 5.

2. ade2::sgRNA+URA3

This system aimed to test whether an associated 'cargo' gene could be spread with the minimal drive element. Its design is depicted in Fig. 3a, and results are shown in Fig. 3b. The related experiment measured drive presence via a visible phenotype (red pigment). In total, 60 haploids were red, or $D = 60$, out of 60 total alleles, $T = 60$. Thus:

$$P = 1$$

3. sgRNA+ABD1

The sgRNA+ABD1 drive system tested the ability to target a recoded essential gene. Its design is depicted in Fig. 3c, and results are discussed in the text (first full paragraph on pp. 1252). The presence of the drive was measured via sequencing of the ABD1 locus. In total, haploids were found to have the drive, $D = 72$, out of 72 counted, $T = 72$.

$$P = 1$$

4. cas9+sgRNA

The first example of an 'autonomous' drive in the paper, this system is depicted in Fig. 5a. It consisted of a gRNA and cas9 together targeting the ADE2 locus (recoded due to safety/containment considerations). The fractional abundance of drive allele was measured by performing qPCR on diploid offspring from wild-type/drive haploid matings; the corresponding data is found in Fig. 5b. The fractional abundance of the drive allele was measured to be $> 99\%$, so $P > 0.99$, as for the first construct above.

$$P > 0.99$$

5. ADE2+sgRNA+cas9

This system is DiCarlo et al.'s example of a 'reversal' drive, designed to target and overwrite the autonomous drive (cas9+sgRNA, directly above). The system is depicted in Fig. 5c. The drive efficiency was measured in the same way as that for the cas9+sgRNA drive (qPCR to calculate fractional abundance of the overwriting drive allele in diploid offspring from haploid matings). The fractional abundance was calculated to be $> 99\%$, so $P > 0.99$, as above.

$$P > 0.99$$

Fruit flies, Gantz et al., (2015)

Gantz et al. constructed an X-linked drive construct targeting the (X-linked) *yellow* locus in *Drosophila melanogaster* and acting in the early embryo [2]. The drive functions to knock out the *yellow* gene, which produces a yellow-body phenotype, denoted $y-$, due to lack of black melanin pigment formation. The wild-type phenotype is referred to as $y+$. Females with < 2 copies of the drive or males with 0 copies should appear $y+$, while females with 2 copies of the drive or males with 1 copy should appear $y-$. The related data is found in Fig. 2E and Table S1.

Two sets of crosses were performed: (i) drive-males with wild-type females, and (ii) drive-females with wild-type males. To tabulate the allele counts D and T, we discuss the two crosses separately.

First, cross (i): In this cross, male offspring could not have possibly inherited a drive allele nor received one through conversion. This is because the only allele they could have inherited from the

drive-male parent was the Y chromosome, but the drive is X-linked. Thus we do not consider male offspring in the total. As for female offspring, these should inherit exactly one drive allele and one wild-type allele prior to conversion. Then the adult female individuals should appear $y-$ if and only if drive-mediated conversion was successful. Thus we add exactly two alleles for each female offspring toward the total allele count, while we add one or two drive alleles to the drive allele count if the adults are $y+$ or $y-$, respectively. This yields $D_{\male} = 40\times 2 = 80$ and $T_{\male} = 40\times 2+1\times 2 = 82$. The drive efficiency for this cross is $P_{\male} = 2D_{\male}/T_{\male} - 1 = 0.951$.

Second, cross (ii): In this cross, male offspring are again uninformative, since each should inherit exactly one drive allele from the female parent and one Y allele from the male wild-type parent. Thus we ignore male offspring in our counting. Female offspring, on the other hand, should all begin as WD embryos, with $y+$ phenotypes. Then adults are $y-$ if and only if they have undergone drive-mediated conversion. Thus we count two alleles for every female offspring in the total, one drive allele per $y+$ adult and two drive alleles per $y-$ adult. This yields $D_{\female} = 203\times 2+1\times 6 = 412$, and $T_{\female} = 203\times 2 + 6\times 2 = 418$. The drive efficiency for this cross is thus $P_{\female} = 2D_{\female}/T_{\female} = 0.971$.

We then consider crosses (i) and (ii) together to calculate the overall drive efficiency. This yields:

$$P = 2\frac{D_{\male} + D_{\female}}{T_{\male} + T_{\female}} - 1 = 2\frac{80 + 412}{82 + 418} - 1 = 0.968$$

Fruit flies, Champer et al., (2017)

Champer et al. constructed two CRISPR gene drive constructs in *D. melanogaster* [3]. The first resembled the *vasa* promoter-driven construct from Gantz et al., discussed in the section immediately above. An important addition, however, was a DsRed fluorescent protein as payload in the drive construct, which allows the drive to be detected in heterozygotes, as its red fluorescent phenotype is dominant. The second construct used the *nanos* promoter, which has been shown to restrict drive function to the germline and is expected to produce less toxicity (and thus a lower fitness cost associated with the drive construct).

1. *vasa* construct

This construct was similar to the one studied by Gantz et al., discussed above. The construct targets the X-linked *yellow* gene. Disruption of the gene produces a recessive yellow phenotype, while the drive itself carries a DsRed payload, producing a dominant red fluorescent eye phenotype. To assess the construct's homing efficiency, wild-type males were crossed with heterozygous DW females. In this setup, all progeny should exhibit the red eye phenotype if the drive is perfectly efficient, while roughly 50% of progeny should exhibit the red eye phenotype in the absence of conversion. Here we count toward the total number of drive or susceptible alleles one allele per male offspring and one allele per female offspring, since in either case only one allele is inherited from the drive parent. Toward the number of drive alleles, we count one per offspring if the offspring displays the DsRed phenotype and zero otherwise. This data is shown in Table 2B of the Champer et al. (2017) study. We count as follows: $D_{\female} = 909 + 4 = 913$ (*i.e.*, the number of drive alleles counted over female offspring), $T_{\female} = 909 + 4 + 316 = 1229$, $D_{\male} = 953$, $T_{\male} = 953 + 265 + 3 = 1221$. Then we obtain:

$$P = 2\frac{D_{\male} + D_{\female}}{T_{\male} + T_{\female}} - 1 = 2\frac{953 + 913}{1221 + 1229} - 1 = 0.523.$$

2. *nanos* construct

This construct is essentially the same as the *vasa* construct, except that it uses a different promoter and targets a different sequence in the *yellow* gene (the coding sequence, rather than the promoter as in the previous construct). The data is found in Table 1B of the Champer et al. (2017) study. We count potential drive alleles and total alleles as above. Our count is as follows: $D_{♀} = 290 + 100 + 108 = 498$, $T_{♀} = 290 + 100 + 108 + 119 + 10 + 9 = 636$, $D_{♂} = 594$, $T_{♂} = 594 + 11 + 103 + 2 = 710$. We obtain:

$$P = 2\frac{D_{♂} + D_{♀}}{T_{♂} + T_{♀}} - 1 = 2\frac{498 + 594}{710 + 636} - 1 = 0.622.$$

Additional data

The constructs described above were then tested in a variety of additional *D. melanogaster* lines, detailed in Table 3 of that work. The authors' efficiency calculations are detailed in the S1 Dataset. For the vasa construct (2 lines), the minimum is $P = 0.37$, and the maximum is $P = 0.53$. For the nanos construct (7 lines), the minimum is $P = 0.40$, and the maximum is $P = 0.63$.

Mosquitoes, Gantz et al., (2015)

In this study, Gantz et al. constructed an autonomous CRISPR-based gene drive system in the malaria vector mosquito *Anopheles stephensi* [4]. The construct comprises two effector genes with anti-*Plasmodium falciparum* activity, a dominant marker gene (DsRed), and the CRISPR components (Cas9 with a single gRNA), spanning roughly 17 kb. The construct targets the *kynurenine hydroxylase*^{white} (*kh*^{w}) locus, which has a recessive white-eye phenotype. The effect of this targeting is that drive/wild-type heterozygotes display a DsRed phenotype, while drive homozygotes display both DsRed and white eyes.

While this one construct was made and studied, it exhibited differential transmission between lines founded by drive males/wild-type females and drive-females/wild-type males. More specifically, lines in which drive alleles are inherited only through male parents display drastically higher drive efficiencies than lines in which the drive allele is inherited at some point via a female parent. To explain this discrepancy, the authors propose a model whereby in crosses between transgenic females and wild-type males, maternal deposition of Cas9 in eggs results in NHEJ-mediated disruption of the paternally derived wild-type chromosome in the early embryo. Crosses between transgenic males and wild-type females, on the other hand, do not see Cas9 deposited in the early embryo, and Cas9 cutting is better contained to the later germline, where HDR is more efficient.

To account for this discrepancy, we choose to consider these two cases separately and report homing efficiencies for each.

1. Transgenic male lines

Here we consider all offspring (larvae + adults) whose drive alleles (or potentially-inherited drive alleles) have been passed down only through male ancestors. This includes all offspring from the male-founder crosses in Table 1 of the main text (10.1 G_2♂ and 10.2 G_2♂), as well as crosses 6 and 8 in Table 2 (also Fig. 3). We choose to compile all alleles from each of these crosses together to calculate an average efficiency across all available data. Because the constructs are on autosomes, we treat male offspring and female offspring identically, and we count toward the total allele count, T, one allele from each offspring (since at most one drive allele can be inherited in each cross), and

G_3 crosses	D	T	Reference
10.1 G_2×WT, larval	829	832	Table S3
10.2 G_2×WT, larval	3060	3085	Table S4
10.1 G_2×WT, adult	833	836	Table S5
10.2 G_2×WT, adult	1258	1274	Table S6
Total	5980	6027	—

G_4 crosses	D	T	Reference
Cross 6, larval	949	955	Table S7
Cross 8, larval	609	628	Table S8
Cross 6, adult	882	888	Table S10
Cross 8, adult	565	583	Table S11
Total	3005	3054	—

Table S2: Gantz et al., *An. stephensi* transgenic male lines. (left) Phenotypes of G_3 progeny. (right) Phenotypes of G_4 progeny.

G_4 larvae	D	T	Reference
Cross 1	28	48	Table S7
Cross 2	332	635	Table S7
Cross 3	204	324	Table S8
Cross 4	372	632	Table S8
Total	936	1639	—

G_4 adults	D	T	Reference
Cross 1	19	35	Table S10
Cross 2	306	554	Table S10
Cross 3	169	272	Table S11
Cross 4	1430	2500	Table S11
Total	1924	3361	—

Table S3: Gantz et al., *An. stephensi* transgenic male lines. (left) Phenotypes of G_4 larvae. (right) Phenotypes of G_4 adults.

we count toward the drive allele total, D, one allele for each $DsRed^+$ individual observed, since this is a dominant marker for the drive. Finally, we consider both larvae and adults identically, as conversion is anticipated to have occurred before this stage, and results are similar between adults and larvae. Values of D and T for each cross are displayed in Table S2.

To obtain an average efficiency for the construct, we sum the values of D and T across all crosses in Table S2. We obtain:

$$P = 2\frac{8985}{9081} - 1 = 0.979.$$

2. Transgenic female lines

To understand the effect of maternal Cas9 deposition, we count all offspring (larvae + adults) from crosses such that the any (potentially) inherited drive allele has been inherited via a female parent at least once. This includes no G_3 offspring, as the drive alleles present in G_2 parents were inherited from G_1 males. Thus we include only G_4 offspring of G_3 parents, specifically Crosses 1-4, and as for the transgenic male lines, we sum both larval and adult crosses. Values of D and T for each cross are displayed in Table S3. Summing the values in Table S3 yields:

$$P = 2\frac{2860}{5000} - 1 = 0.144.$$

Mosquitoes, Hammond et al., (2015)

In this study, the authors construct three CRISPR-based gene drive systems in the malaria vector *An. gambiae*, each targeting a different gene with a recessive female sterility phenotype upon disruption [5]. These are examples of suppression drives whose purpose is to reduce or eradicate wild

populations. Each drive construct carries a copy of Cas9, a single guide RNA, and red fluorescent protein (RFP) which has a dominant fluorescent phenotype. Each construct targets one of three female fertility genes, referred to as AGAP011377, AGAP005958, and AGAP007280, but otherwise they are identical.

To determine homing efficiency, drive-heterozygotes were crossed with wild-type homozygotes, and offspring were scored visually for the presence of the dominant marker RFP gene. Thus in our tabulations, we count one allele per individual toward the total, T, and we count one allele per RFP$^+$ individual toward the drive allele count, D. Furthermore, the outcrosses were performed over several generations. To obtain average homing efficiencies, we sum drive alleles and total alleles over G_2, G_3, G_4, and G_5 generations, when applicable. (Some constructs were tested over more generations than others.) This data is found in Table 2 in the study. Furthermore, we sum across male- and female-drive parent crosses, since we would expect these to behave identically with respect to homing, given that the female drive parents are capable of producing offspring.

1. AGAP011377

This construct was studied over generations G_2 to G_5 in Table 2. The total number of relevant alleles resulting from crosses between drive-male parents and wild-type females was $T_{♂} = 636 + 1631 + 1654 + 505 = 4426$, while the male drive total was $D_{♂} = 581 + 1442 + 1550 + 491 = 4064$. The female total was $T_{♀} = 60 + 92 + 142 = 294$, and the female drive total was $D_{♀} = 55 + 70 + 121 = 246$. The average efficiency is then:

$$P = 2\frac{D_{♂} + D_{♀}}{T_{♂} + T_{♀}} - 1 = 2\frac{4064 + 246}{4426 + 294} - 1 = 0.826.$$

2. AGAP005958

This construct was studied over generations G_2 and G_3. There were no offspring from female-drive crosses to wild-type due to the low fertility of these individuals. The total was $T = 1689 + 278 = 1967$, and the drive total was $D = 1654 + 268 = 1922$. The efficiency is thus:

$$P = 2\frac{D}{T} - 1 = 2\frac{1922}{1967} - 1 = 0.954.$$

3. AGAP007280

This construct was studied over generations G_2 and G_3. The male total was $T_{♂} = 1383 + 505 = 1888$, and the male drive total was $D_{♂} = 1377 + 499 = 1876$. The female total was $T_{♀} = 257$, and the female drive total was $D_{♀} = 255$. The efficiency is:

$$P = 2\frac{D_{♂} + D_{♀}}{T_{♂} + T_{♀}} - 1 = 2\frac{1876 + 255}{1888 + 257} - 1 = 0.987.$$

2 Additional results

In this Section, we further explore various aspects of our model which could conceivably affect drive invasiveness and present additional results from numerical simulations. In particular, we study the effects of varying the following quantities: (i) population size, (ii) standing genetic variation, (iii) drive fitness and homing efficiency, (iv) the number of adult offspring produced per mating event, and (v) inbreeding.

2.1 Population size

Throughout the main text, we present results from simulations which assume populations of size $N = 500$. We claim that $N = 500$ is a reasonable approximation for the dynamics in the large-population limit, which is the relevant regime for widespread invasion or for species with very large population sizes, e.g., mosquitoes. Here we briefly evaluate this claim.

Figure S1 recreates Figure 1e from the main text with additional population sizes overlaid: $N = 1000$, 2500, 5000, and 10000. The distributions narrow for larger N until plateauing at roughly $N = 5000$. However, the central tendencies show little change with increasing N.

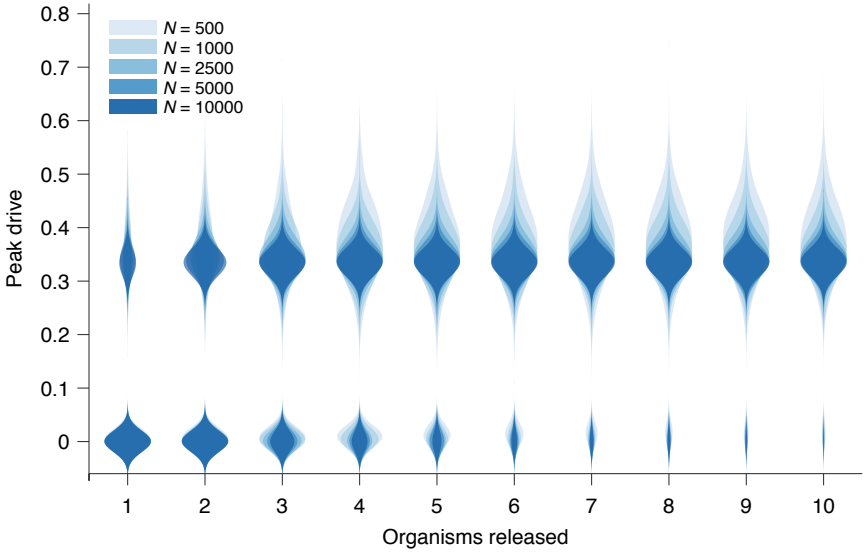

Figure S1: Peak drive distributions for variable release and population sizes. Parameters are chosen to correspond to Figure 1e in the main text: $P = 0.5$, $f = 0.9$ and neutral resistance. Population sizes are, from light to dark, $N = 500, 1000, 2500, 5000, 10000$. Note that $N = 500$ corresponds exactly to Figure 1e in the main text. Each distribution corresponds to 10^3 simulations.

2.2 Standing genetic variation

Several recent studies have explored the effect of pre-existing drive resistant alleles in a population brought about by standing genetic variation (SGV) at the target locus [6, 7]. These studies developed deterministic models and showed that pre-existing resistant alleles—presumably neutral—should rapidly outcompete costly drives due to selection, resulting in rapid drive extinction. The study by Drury et al. [7] used sequencing to quantify this standing variation in diverse populations of flour beetles and found resistance-conferring mutations to exist at a wide range of frequencies, from 0 to 0.375, with an average of roughly 0.1.

However, these studies were primarily concerned with long-term outcomes following drive release, in which case resistance certainly outcompetes the drive. For our purposes, however, we are concerned with the intermediate time regime in which the dynamics of resistance are less clear. Moreover, these studies employed deterministic models, whereas our model is stochastic. Here, we seek to understand the effect of SGV in our model.

To incorporate SGV, we simply alter the initial conditions: rather than introducing i drive homozygotes into a population of $N - i$ wild-type homozygotes, we introduce i drive homozygotes into

a population consisting of j resistant homozygotes (we choose resistant homozygotes for simplicity, since they rapidly go to Hardy-Weinberg equilibrium following release) and $N-i-j$ wild-type homozygotes. Figure S2 shows the effect of SGV on peak drive for pre-existing resistance frequencies up to 0.5.

We find that the effect of SGV is to linearly decrease the mean peak drive ($R^2 = 0.996$). Our intuition for this result is as follows. Because the population is well-mixed, the effect of resistance is simply to decrease the size of the population that is susceptible to the effects of the drive. This can be roughly viewed as linearly scaling the drive-frequency axis. For example, if the population has a 0.1 frequency of resistant alleles immediately prior to release, then the population that is susceptible to drive is roughly 90% of the census population size, and the drive undergoes its usual dynamics within this subpopulation. There are of course complications to this simplistic explanation, e.g., selection increasing the size of the resistant population and diploidy mixing resistant and drive alleles. Furthermore, the linear relationship only holds for sufficiently low levels of SGV. In our example here, the relationship holds to roughly 0.5 initial resistance frequency. However, this is still higher than would be anticipated for drives engineered to spread in the wild.

Overall, our results suggest that a high level of SGV would be required to protect against drive invasion. In our conservative example (Fig. S2) assuming 0.5 homing efficiency, 0.9 drive fitness, and neutral resistance, pre-existing resistance of greater than 0.5 frequency is required to contain peak drive to below 10% of the population, compared to 35% in the absence of SGV.

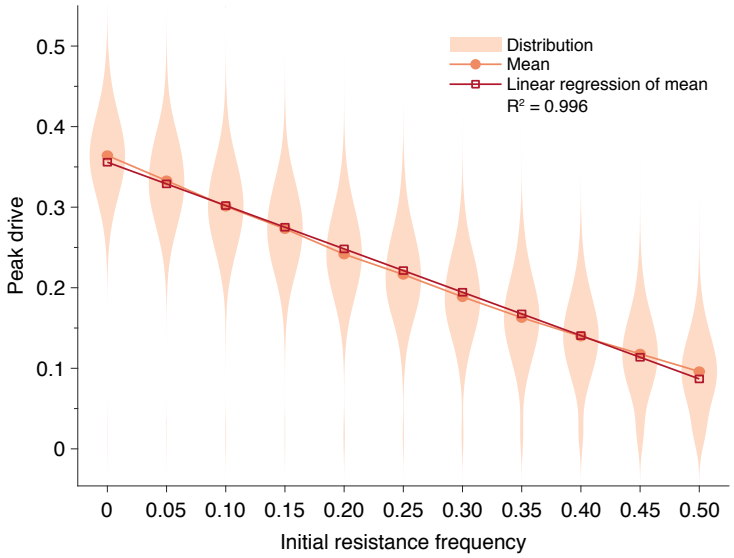

Figure S2: Pre-existing drive-resistant allele frequency linearly decreases peak drive. Distributions (violin plots), means (orange, circles) and linear regression of the mean values (red, squares). Parameters are chosen to correspond to Figure 1e in the main text: $P = 0.5$, $f = 0.9$, neutral resistance, $N = 500$. Each distribution corresponds to 5000 simulations.

2.3 Offspring number distribution

In the model presented in the main text, we assume that each mating produces one offspring. However, a variety of application-relevant species are known to produce many offspring per mating. For example, female *Anopheles gambiae* mosquitoes can lay hundreds of eggs per lifetime [5]. It is not clear, *a priori*, how varying the offspring number distribution in our model would affect the

results presented in the main text. Thus we here analyze a simple extension of the model which allows us to vary the number of offspring following a given mating event.

To begin, recall our model from the main text. We consider a population of constant size N with the following process: At each time-step, two individuals are chosen for mating; an offspring is sampled according to the parental genotypes; a third individual is chosen for removal from the population, and the parents' offspring takes its place. (We implicitly assume that these offspring are only the offspring which successfully reach adulthood, i.e., reproductive age.) We now add a new parameter, k, which determines number of (adult) offspring produced by a mating pair. The process proceeds as before, except now k offspring are independently sampled from the parental genotypes, and k individuals are chosen uniformly (without replacement) for removal from the population. Clearly the model presented in the main text is the special case $k = 1$.

Note that this parameter k is not equivalent to brood size, clutch size, egg batch size, etc.—values often considered in the ecological literature—in that k describes the number of offspring produced per mating which successfully attain reproductive age. This number can of course be much lower than these other parameters due to death during juvenile life stages. We provide an example calculation for this parameter in *An. gambiae* at the end of this section.

We now argue that increasing the number of offspring per mating, k, corresponds to decreasing the effective size of the population, N_e. We omit rigorous proof here, but we provide a formula for the effective population size in our model and present numerical simulations as support. To begin, Hill showed in 1972 that the variance effective population size in the standard Moran model is [8]

$$N_e = \frac{4N}{2 + \sigma_X^2}. \tag{1}$$

Here N is the census population size, and σ_X^2 is the variance in the distribution of the total number of offspring produced by an individual over the course of its lifetime (*i.e.*, its lifetime reproductive success). It was proven that this formula holds both for the Wright-Fisher model with discrete generations and for the Moran model with overlapping generations, provided that σ_X^2 is the same and that the total number of individuals entering the population in each generation is equal [8]. Our model meets both of these requirements—indeed, the only difference is that two parents are chosen to sample offspring types, rather than one, and this has no bearing on the number of offspring produced—so we conjecture that Eq. (1) holds for our case as well.

To proceed, we calculate σ_X^2 for our extended model and employ the variance effective population size given by Eq. (1). Consider one particular individual in the population, and let $t = 1, 2, \ldots$ count time-steps. As described, in each step, k individuals are uniformly sampled (without replacement) for removal. Thus, an individual has probability k/N of dying in each step. Its lifespan, T, is thus geometrically distributed, $T \sim \text{Geometric}(k/N)$.

Next, let X be a random variable describing the number of offspring an individual produces in its lifetime, so that $X|T$ is the number of such events given that the individual survives T time-steps. Because each mating event is independent, $(X|T) \sim k \cdot \text{Bin}(T, 2/N)$. The success probability derives from the fact that two individuals are chosen for mating in each time-step and that the process is neutral. Thus,

$$\mathbb{E}X = \mathbb{E}\mathbb{E}\left[X \mid T\right] = \mathbb{E}k(2/N)T = k(2/N)N/k = 2$$

and

$$\begin{aligned}
\text{Var}(X) &= \mathbb{E}\text{Var}(X \mid T) + \text{Var}(\mathbb{E}(X \mid T)) \\
&= \mathbb{E}k^2T(2/N)(1 - 2/N) + \text{Var}(k(2/N)T) \\
&= kN(2/N)(1 - 2/N) + (2k/N)^2N(N - k)/k^2 \\
&= 4 + 2k(N - 4)/N.
\end{aligned}$$

Returning to the variance effective population size expression in Eq. (1), we obtain for our model:

$$N_e = \frac{4N}{2k+6}. \tag{2}$$

Note that in the case $k = 1$ we recover $N_e = N/2$, which is the variance effective population size for the standard Moran model.

In Fig. S3, we present peak drive distributions (as in Figs. 1E and S1) for varying values of k with the effective population size, N_e, and effective release size, i_e, both determined by Eq. (2), held constant. In this case we used $N_e = 250$ and $i_e = 8$, which correspond to $N = 500$ and an initial release of $i = 16$ in our standard model with $k = 1$. The peak drive distributions for all values of k studied are approximately identical. This suggests that the dynamics for larger k can indeed be inferred from the standard model with $k = 1$ and population/release sizes appropriately scaled via Eq. (2). An immediate consequence of this result is that releases of organisms which have many offspring (e.g., mosquitoes) are effectively smaller than would be expected from simply counting. For example, an organism which typically has 100 offspring would need a release size of roughly 258 to surpass the 10-individual initial release threshold we have observed. Note that the 10-individual threshold discussed throughout the text is the census release size; the effective release size is $i_e = 5$.

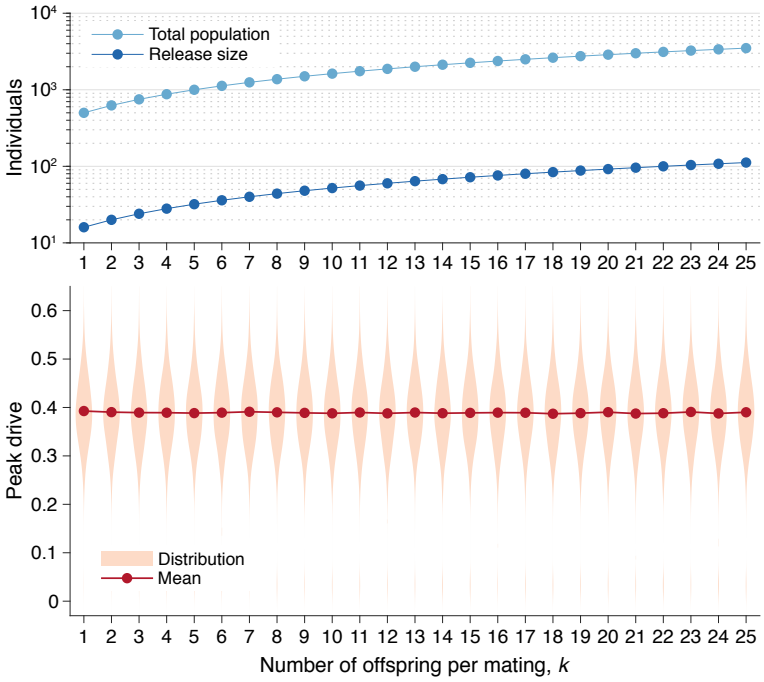

Figure S3: Peak drive distributions for varying numbers of offspring per mating with effective population and release sizes held constant. (top) Population and release sizes used in the simulations below. For the case $k = 1$, we use our usual population size of $N = 500$ with an initial release of $i = 16$ drive homozygotes. According to eq. (2), the effective total population and release sizes in this case are $N_e = 250$ and $i_e = 8$. For other values of k, we use values of N and i which maintain constant effective population and release sizes: $N = N_e(2k + 6)/4$ and $i = i_e(2k + 6)/4$. These values are plotted: N (light blue) and i (dark blue). (bottom) Peak drive distributions assuming values of N and i as in the above plot. All employ $P = 0.5$, $f = 0.9$, and neutral resistance. Each distribution includes 5000 simulations.

In Fig. S4, we recalculate the distributions in Fig. S3 holding the *actual* population and release sizes constant, rather than their effective values. Two effects are apparent. First, the decrease in effective population size, N_e, leads to greater variation in peak drive among simulations that invade, *i.e.*, the distribution centered around ≈ 0.4 widens. Second, the decrease in effective release size, i_e, leads to a greater probability of simulations immediately going extinct, *i.e.*, the relative mass of the mode centered around ≈ 0 increases. In sufficiently large populations the first effect would be less pronounced—see Fig. S1—while the second effect should apply for any small release.

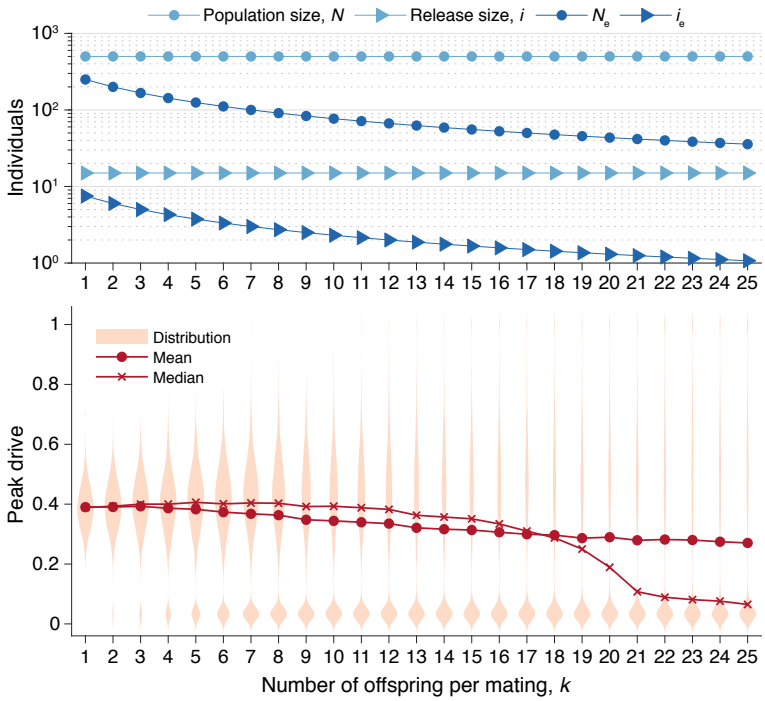

Figure S4: Peak drive distributions for varying numbers of offspring per mating with census population and actual release sizes held constant. (top) Population and release sizes used in the simulations below. Actual population size, N (light blue, circles) and actual release size, i (light blue, triangles). Note that $N = 500$ and $i = 15$ are constant. Effective values calculated via Eq. (2): population size, N_e (dark blue, circles) and release size, i_e (dark blue, triangles). (bottom) Peak drive distributions for simulations using indicated values of k and population and release sizes as depicted above. Compare with Fig. S3 which holds the *effective* population and release sizes constant, whereas here we hold the *census* population and release sizes constant. All simulations employ $P = 0.5$, $f = 0.9$, and neutral resistance. Each distribution includes 5000 simulations.

Finally, as an example, we provide an estimate of our model's k parameter for a particularly relevant species, *An. gambiae*. To do this, we find the typical size, n, of egg batches laid by females following a particular mating event; then we estimate the total number of these which survive to adulthood using parameters from the literature.

The first number, n, varies according to a variety of environmental and ecological factors [5, 9], so we assume a large but reasonable value in order to avoid underestimating our parameter k. For this, we assume that $n \approx 186$, which is roughly the highest value observed by Hammond et al. in the CRISPR drive study [5] and is in line with previous field work [9].

To estimate the survival probability for each egg to adulthood, we employ the method and parameters presented by Deredec et al. [10] Each egg goes through three juvenile stages before

reaching adulthood—the egg stage, the larva stage, and the pupae stage. We denote the probabilities of surviving each of these stages by θ_0, θ_L, and θ_P, respectively. The probability of a particular egg reaching adulthood is then $p = \theta_0\theta_L\theta_P$. These parameters were estimated to be $\theta_0 = 0.831$, $\theta_L = 0.076$, and $\theta_P = 0.831$. Thus we have $p = 0.0525$.

Given this formulation, the number of eggs laid per mating event which reach adulthood is distributed according to $\text{Bin}(n, p)$. We take the mean of this distribution to obtain:

$$k \approx np = 9.76.$$

Therefore, while *An. gambiae* females exhibit large egg batch sizes, the value of k for our model is much lower—indeed, low enough that the central tendency of the peak drive distribution remains roughly unchanged in Fig. S4.

2.4 Drive fitness and homing efficiency

In the main text, we study various values of the homing efficiency, P, but we perform less exploration of the drive fitness, f. This is motivated primarily by the abundance of data for the former—see Table 1 in the main text—and the lack of data for the latter. Here we comprehensively explore the effect of both parameters. In particular, we consider 51 values of each parameter: $P \in [0, 1]$ and $f \in [0.5, 1]$, both evenly spaced, for a total of 2,601 parameter pairs. For each pair, the average peak drive is calculated over 100 simulations, and the results are shown in Figure S5.

We find that maximum drive frequencies of greater than 0.3 are common across a wide range of drive fitness values. In particular, for our lower-bound estimate of empirical drive efficiency ($P = 0.5$), drives can confer fitness costs as high as 20% before the peak drive drops below 0.3. For more typical empirical efficiencies ($P > 0.8$), the peak drive is typically greater than 0.5 even for costly drives ($f \approx 0.7$), and low-cost drives ($f > 0.9$) have peak drive of greater than 0.9.

It is important to note that the peak drive and likelihood of invasion deemed socially acceptable for accidental release would likely be lower than those discussed above. With this in mind, our simulations suggest that if a drive is initially favored by selection (*i.e.*, if it lies above the boundary in Fig. S5), then it will almost certainly reach a maximum frequency greater than 0.1. While acceptable levels of peak drive are as-yet unknown and will likely vary between species, applications, jurisdictions and so on, spread to this extent will likely surpass it.

2.5 Inbreeding

Since the drive functions only in heterozygotes, inbreeding in a population—which in effect reduces the frequency of heterozygotes—would be expected to impact drive invasiveness. Indeed, this has been shown in recent theoretical studies by Bull [11] and Drury et al. [7] Thus we here extend our well-mixed model to include inbreeding and study its effect.

For simplicity, we consider a partial selfing model. In each update step of our process (see Fig. 1c in the main text), we typically choose two parents for mating with probabilities proportional to their fitnesses. To include selfing, we instead choose the first parent as usual, with probability proportional to its fitness. We then choose the first parent as the second parent as well with probability s; or, with probability $1 - s$, we choose a second parent from the remaining population, with probability proportional to its fitness. Note that the fitness of each offspring is determined entirely by its genotype and does not account for inbreeding depression. Implicitly, we thus consider the case of zero inbreeding depression. As this effect helps protect against drive invasion, we essentially consider the worst-case scenario for drive containment [11].

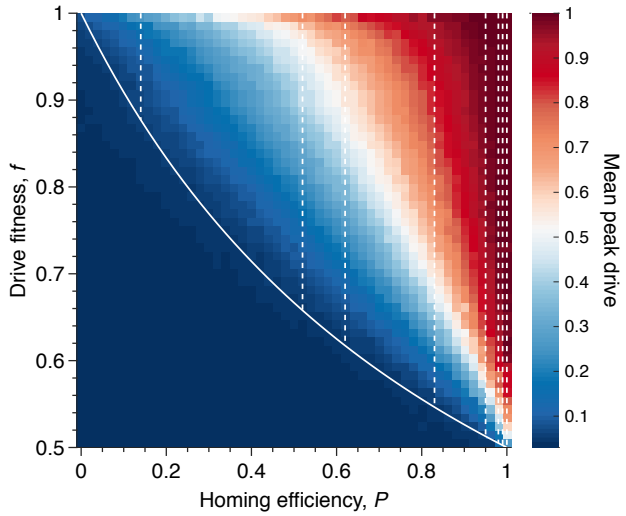

Figure S5: Mean peak drive for varying homing efficiency, P, and drive-individual fitness values, f (*i.e.*, individuals with genotypes WD, DD, and DR). The solid white line shows the boundary from Fig. 1b indicating whether the drive is initially favored by selection. The drive is only expected to invade based on deterministic models if the fitness/homing efficiency pair lie above the boundary. The dashed white lines indicate the empirically measured homing efficiencies from Table S1 and Fig. 1b in the main text. Each point in the grid (51×51) depicts an average of 100 simulations. Parameters used include a population size of 500, with an initial release of 15 drive homozygotes to ensure that trajectories establish. Neutral resistance is assumed throughout with no standing genetic variation.

Using our extended model, we then computed peak drive distributions for values of s between 0 and 1 and for the three values of P explored in the main text: $P = 0.15, 0.5, 0.9$. The results are shown in Fig. S6. We find that a fairly high degree of selfing is required to impact the peak drive distribution in a meaningful way. For highly effective drive, $P = 0.9$, the mass of the upper mode in the frequency distribution is larger than the lower mode until roughly $s \approx 0.75$. For conservative drive, $P = 0.5$, this occurs at roughly $s \approx 0.6$, and for ineffective drive there is little change, as the maximum frequency begins very near zero. To compare with previous results, we can consider the inbreeding coefficient rather than the selfing probability. In our model, the inbreeding coefficient, F, is given by $s/(2-s)$. Thus highly effective drive can tolerate inbreeding of $F \approx 0.6$ and conservative drive can tolerate $F \approx 0.43$.

2.6 Comparison with deterministic model

To show that the deterministic ODE solutions provide reasonable approximations to the typical behavior of our stochastic mode, we overlay numerical solutions to the ODEs for the systems studied in Fig. 1d of the main text. The results are shown in Fig. S7.

Throughout we have assumed that resistance is neutral with respect to the wild-type. This assumption is biologically realizable as resistance is conferred by changing sequence homology to the drive's gRNA—something that could be achieved with synonymous codon substitutions, for example. In practice, some resistance mutations could be costly and those that are neutral could be rare. However, assuming resistance is always neutral represents the worst-case scenario for drive invasiveness, as resistance can increase in frequency without being selected against with respect to

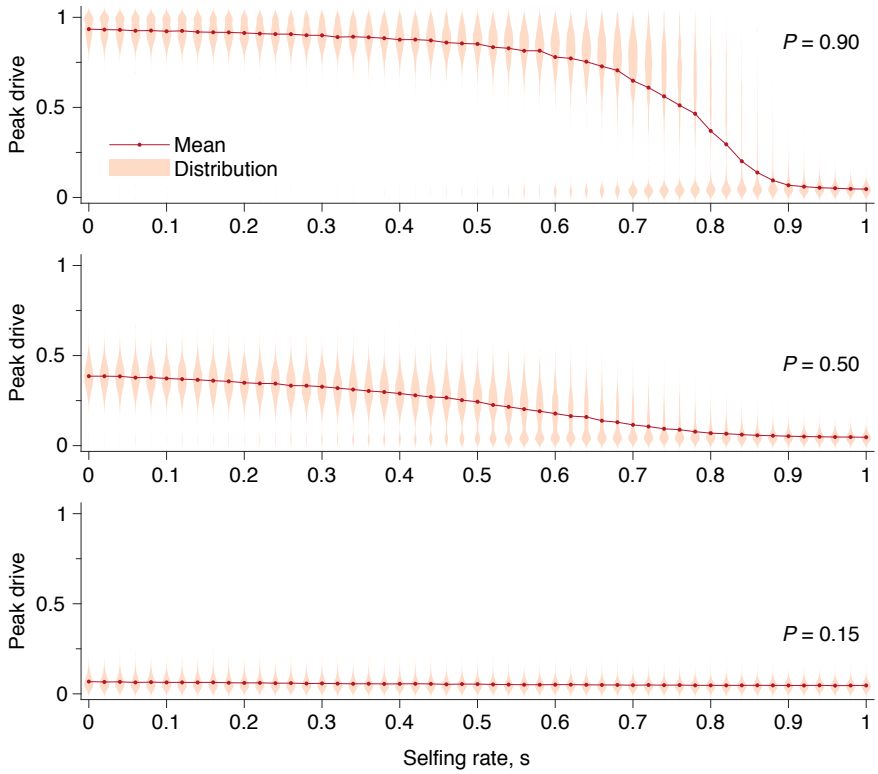

Figure S6: Peak drive distributions and means for varying selfing rates in our partial selfing model. (top) Effective drive, $P = 0.9$. (middle) conservative drive, $P = 0.5$, and (bottom) constitutive drive, $P = 0.15$. Each distribution comprises 1000 simulations. Parameters used include a population size of 500 with an initial release of 15 drive homozygotes. Neutral resistance is assumed throughout with no standing genetic variation, and the offspring number per mating is $k = 1$.

the wild-type.

When resistance is no longer assumed to be neutral, other interesting dynamics can occur [12]. In particular, when resistance is costly with respect to the wild-type, but not so costly as the drive and its cargo, the dynamics resemble the Rock-Paper-Scissors game. This allows the drive to avoid extinction indefinitely.

2.7 Analytic formulae for the escape probability in structured populations

We consider a deme structured population, where each subpopulation has size N and there are n demes. We define a Moran-type process, where in each time step either a reproduction or migration event takes place (illustrated in Fig. S8). A reproduction event occurs with probability $1 - m$ and a migration event occurs otherwise. If a reproduction occurs, then a subpopulation is selected proportional to the square of its total fitness. Next, two individuals in the subpopulation are selected proportional to their fitnesses and they produce an offspring according to the mechanism in the main text. Finally, another individual from the subpopulation is chosen uniformly at random for death. If a migration event occurs, then an individual is selected uniformly at random and migrates to a new subpopulation uniformly at random. We denote the proportion of genotype α at time t in the initial subpopulation by P_t^α.

The process begins with i drive homozygotes and $N - i$ wild-type homozygotes in a single

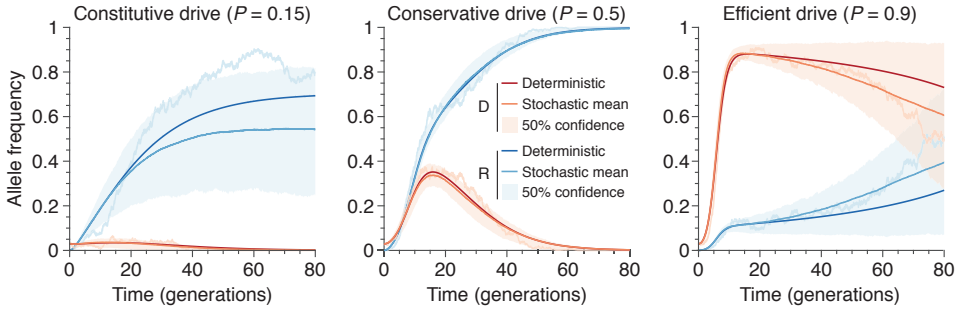

Figure S7: Finite-population simulations of 15 drive individuals released into a wild population of size 500, assuming low ($P = 0.5$) or high ($P = 0.9$) homing efficiencies, as well as a low-efficiency, constitutively active system ($P = 0.15$). Deterministic results (dark lines) and means of 10^3 simulations (medium lines), individual sample simulations (light lines), and 50% confidence intervals (shaded). Drive frequencies red and resistant-allele frequencies blue.

subpopulation. The remaining subpopulations consist only of wild-type homozygotes. Let $\mathcal{E}$ be the event that the frequency of drive alleles reaches 10% in a subpopulation other than where the drive was released, given that i drive homozygotes were released in the initial subpopulation. We assume that i is small with respect to N.

As an aside, note that the choice of 10% is arbitrary—any other percentage (less than the peak drive in the deterministic model, c) would be equivalent if N is large enough. This is clear from Fig. 1e, where either the drive does not invade and so peak drive is roughly equal to the initial frequency or the drive does invade and the peak drive is close to c. This claim is equivalent to stating that the probability that the drive starting at frequency c_0 attains frequency c_1 (such that $c_0 < c_1 < c$) before going extinct tends to 1. This behavior is typical of Moran-type models, since the extinction probability of i drive homozygotes rapidly approaches 0, even in an infinite population, as i increases [13]. Specifically, if we have $i = c_0 N$, then the extinction probability approaches 0 as N becomes large, and moreover, if the drive does not go extinct, then it behaves almost deterministically and will reach frequency c and thus also c_1.

Returning to approximating the probability of $\mathcal{E}$, note that for $\mathcal{E}$ to take place a drive allele has to migrate from the initial subpopulation *and* this allele has to survive stochastic fluctuations and avoid extinction in its new subpopulation. The drive alleles do not last indefinitely in the initial population. We denote the random time at which the drive alleles go extinct by T. As long as the initial drives do not go extinct due to stochastic fluctuations, the frequency of the drive increases rapidly, as it outcompetes the wild-type. Concurrently, resistant alleles are produced that eventually push the drive to extinction. This means that the drive has a finite time to migrate to other subpopulations. Although this process is stochastic it shows fairly deterministic behavior once there are a sufficient number of drive alleles (see Fig S7)—that is, if the drive avoids immediate extinction. Let $e_{i,j}$, be the probability that the drive survives stochastic fluctuations and avoids immediate extinction when starting with i drive homozygotes and j heterozygotes. Implicitly, here we are assume that $e_{i,j}$ does not depend on whether the heterozygotes are wild-type or resistant heterozygotes. Note that when i or j are $\mathcal{O}(N)$, $e_{i,j}$ is approximately 1, so when $i, j \ll N$, we assume that the probability that the drive migrates is approximately 0. Moreover, since the drive will almost certainly go extinct, there is some time where the frequency of drive alleles is again much less than $\mathcal{O}(N)$. We also assume here that the probability that the drive migrates is approximately 0.

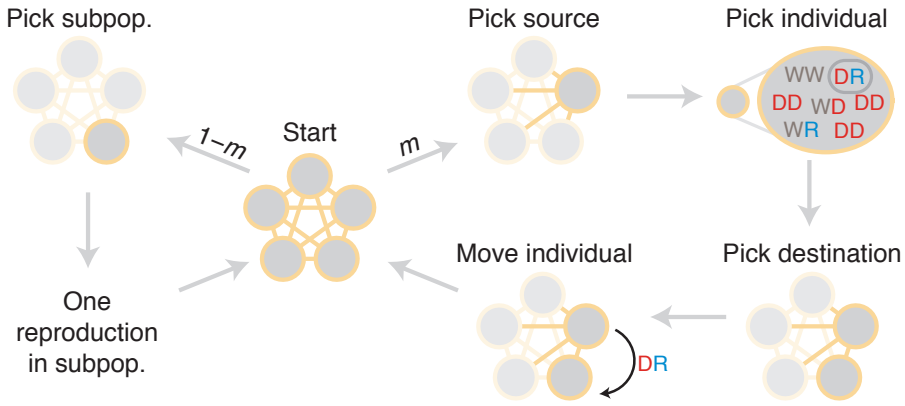

Figure S8: Diagram of simulation scheme. In each time step, a migration occurs with probability m, or a mating happens with probability $1-m$. If a migration occurs, a source population is chosen randomly proportional to its size; an individual is chosen uniformly at random, then a destination is chosen uniformly at random, and the individual is moved. If a mating occurs, the dynamics proceed as in the well-mixed case for a particular subpopulation (Fig. 1c).

At each time step, there is a small probability that the drive migrates from the initial population and invades another subpopulation. To calculate, we first condition on the non-extinction of the initial i drive homozygotes. Second, we note that if the drive does not migrate and avoid extinction in another subpopulation, then it does not do so at any particular time t. Third, we assume that these events for each t are approximately independent. Finally, we numerically solve a deterministic ODE system representing the dynamics [14] to approximate the probability that the drive does not migrate at time t. Thus,

$$\begin{aligned}
\mathbb{P}\{\mathcal{E}\} &= \mathbb{P}\{\mathcal{E} \mid \text{drive avoids extinction}\}e_{i,0} + \mathbb{P}\{\mathcal{E} \mid \text{drive does not avoid extinction}\}(1-e_{i,0}) \\
&\approx \mathbb{P}\{\mathcal{E} \mid \text{drive avoids extinction}\}e_{i,0} \\
&\approx e_{i,0}\left(1 - \prod_{t=1}^{T} \mathbb{P}\{\text{drive does not migrate and invade at time } t\}\right) \\
&= e_{i,0}\left(1 - \prod_{t=1}^{T} (1 - \mathbb{P}\{\text{drive invades} \mid \text{drive migrates at time } t\}\mathbb{P}\{\text{drive migrates at time } t\})\right) \\
&= e_{i,0}\left(1 - \prod_{t=1}^{T} \left(1 - me_{1,0}\mathbb{E}P_t^{DD} - me_{0,1}(\mathbb{E}P_t^{WD} + \mathbb{E}P_t^{DR})\right)\right),
\end{aligned}$$

since if the drive avoids extinction it will invade. Now we substitute the ODE solution $p_t^{\alpha\beta}$ for $\mathbb{E}P_t^{\alpha\beta}$ in the above expression to find that

$$\begin{aligned}
\mathbb{P}\{\mathcal{E}\} &\approx e_{i,0}\left(1 - \exp\left(N\int_0^{T/(1-\lambda)} \mathrm{d}t \log\left(1 - \lambda e_{1,0}p_{(1-\lambda)t}^{DD} - \lambda e_{0,1}\left(p_{(1-\lambda)t}^{WD} + p_{(1-\lambda)t}^{DR}\right)\right)\right)\right) \\
&\approx e_{i,0}\left(1 - \exp\left(\frac{N}{1-\lambda}\int_0^{T} \mathrm{d}t \log(1 - \lambda e_{1,0}p_t^{DD} - \lambda e_{0,1}(p_t^{WD} + p_t^{DR}))\right)\right).
\end{aligned}$$

Here we approximated the product with an integral and used a change of variables.

Note that if $m = \mathcal{O}(1/T)$ and heuristically we replace $\mathbb{E}P_t^\alpha$ in the above expressions with its time average, denoted ϕ^α, then

$$\begin{aligned} & e_{i,0}\left[1-\prod_{t=1}^{T}\left(1-me_{1,0}\mathbb{E}P_t^{DD}-me_{0,1}(\mathbb{E}P_t^{WD}+\mathbb{E}P_t^{DR})\right)\right] \\ & \approx e_{i,0}\left[1-\left(1-\frac{e_{1,0}\phi^{DD}+e_{0,1}(\phi^{WD}+\phi^{DR})}{T}\right)^T\right] \\ & \approx e_{i,0}\left[1-\exp\left(-e_{1,0}\phi^{DD}+e_{0,1}(\phi^{WD}+\phi^{DR})\right)\right]. \end{aligned}$$

Thus, when the migration rate is on the order of the inverse of the drive extinction time, the invasion probability is order 1.

References

[1] DiCarlo, J. E., Chavez, A., Dietz, S. L., Esvelt, K. M. & Church, G. M. Safeguarding CRISPR-Cas9 gene drives in yeast. *Nature Biotechnology* (2015). URL `http://dx.doi.org/10.1038/nbt.3412`.

[2] Gantz, V. M. & Bier, E. The mutagenic chain reaction: A method for converting heterozygous to homozygous mutations. *Science* **348**, 442–444 (2015).

[3] Champer, J. *et al.* Novel CRISPR/Cas9 gene drive constructs reveal insights into mechanisms of resistance allele formation and drive efficiency in genetically diverse populations. *PLOS Genetics* **13**, e1006796 (2017). URL `http://dx.plos.org/10.1371/journal.pgen.1006796`.

[4] Gantz, V. M. *et al.* Highly efficient Cas9-mediated gene drive for population modification of the malaria vector mosquito Anopheles stephensi. *Proceedings of the National Academy of Sciences* 201521077 (2015).

[5] Hammond, A. *et al.* A CRISPR-Cas9 gene drive system targeting female reproduction in the malaria mosquito vector Anopheles gambiae. *Nature biotechnology* (2015). URL `http://dx.doi.org/10.1038/nbt.3439`.

[6] Unckless, R. L., Clark, A. G. & Messer, P. W. Evolution of Resistance Against CRISPR/Cas9 Gene Drive. *Genetics* **205**, 827–841 (2017).

[7] Drury, D. W., Dapper, A. L., Siniard, D. J., Zentner, G. E. & Wade, M. J. CRISPR/Cas9 gene drives in genetically variable and nonrandomly mating wild populations. *Science Advances* **3** (2017). URL `http://advances.sciencemag.org/content/3/5/e1601910`.

[8] Hill, W. G. Effective size of populations with overlapping generations. *Theoretical population biology* **3**, 278–289 (1972).

[9] Yaro, A. S. *et al.* Reproductive Output of Female Anopheles gambiae (Diptera: Culicidae): Comparison of Molecular Forms. *Journal of Medical Entomology* **43**, 833–839.

[10] Deredec, A., Godfray, H. C. J. & Burt, A. Requirements for effective malaria control with homing endonuclease genes. *Proceedings of the National Academy of Sciences of the United States of America* **108**, E874–80 (2011).

[11] Bull, J. J. Lethal gene drive selects inbreeding. *Evolution, Medicine, and Public Health* eow030 (2016). URL `http://emph.oxfordjournals.org/lookup/doi/10.1093/emph/eow030`.

[12] Traulsen, A. & Reed, F. A. From genes to games: Cooperation and cyclic dominance in meiotic drive. *Journal of Theoretical Biology* **299**, 120–125 (2012).

[13] Marshall, J. M. The effect of gene drive on containment of transgenic mosquitoes. *Journal of Theoretical Biology* **258**, 250–265 (2009).

[14] Noble, C., Olejarz, J., Esvelt, K. M., Church, G. M. & Nowak, M. A. Evolutionary dynamics of CRISPR gene drives. *Science Advances* **3** (2017). URL `http://advances.sciencemag.org/content/3/4/e1601964`.